Eur Radiol (2014) 24:913–920
DOI 10.1007/s00330-013-3075-8

BREAST

Clinical application of bilateral high temporal and spatial resolution dynamic contrast-enhanced magnetic resonance imaging of the breast at 7 T

K. Pinker · W. Bogner · P. Baltzer · S. Trattnig · S. Gruber · O. Abeyakoon · M. Bernathova · O. Zaric · P. Dubsky · Z. Bago-Horvath · M. Weber · D. Leithner · T. H. Helbich

Received: 21 August 2013 / Revised: 11 October 2013 / Accepted: 3 November 2013 / Published online: 5 December 2013

Abstract
Objective The objective of our study was to evaluate the clinical application of bilateral high spatial and temporal resolution dynamic contrast-enhanced magnetic resonance imaging (HR DCE-MRI) of the breast at 7 T.
Methods Following institutional review board approval 23 patients with a breast lesion (BIRADS 0, 4–5) were included in our prospective study. All patients underwent bilateral HR DCE-MRI of the breast at 7 T (spatial resolution of 0.7 mm^3 voxel size, temporal resolution of 14 s). Two experienced readers (r1, r2) and one less experienced reader (r3) independently assessed lesions according to BI-RADS®. Image quality, lesion conspicuity and artefacts were graded from 1 to 5. Sensitivity, specificity and diagnostic accuracy were assessed using histopathology as the standard of reference.
Results HR DCE-MRI at 7 T revealed 29 lesions in 23 patients (sensitivity 100 % (19/19); specificity of 90 % (9/10)) resulting in a diagnostic accuracy of 96.6 % (28/29) with an AUC of 0.95. Overall image quality was excellent in the majority of cases (27/29) and examinations were not hampered by artefacts. There was excellent inter-reader agreement for diagnosis and image quality parameters (κ=0.89–1).
Conclusion Bilateral HR DCE-MRI of the breast at 7 T is feasible with excellent image quality in clinical practice and allows accurate breast cancer diagnosis.

Key points
- *Dynamic contrast-enhanced 7-T MRI is being developed in several centres.*
- *Bilateral high resolution DCE-MRI of the breast at 7 T is clinically applicable.*
- *7-T HR DCE-MRI of the breast provides excellent image quality.*
- *7-T HR DCE-MRI should detect breast cancer with high diagnostic accuracy.*

Keywords 7 Tesla · Ultra-high field · High resolution · DCE-MRI · Breast cancer

K. Pinker · P. Baltzer · M. Bernathova · M. Weber · D. Leithner · T. H. Helbich (✉)
Department of Biomedical Imaging and Image-guided Therapy, Division of Molecular and Gender Imaging, Medical University Vienna, Waehringer Guertel 18-20, 1090, Vienna, Austria
e-mail: thomas.helbich@meduniwien.ac.at

W. Bogner · S. Trattnig · S. Gruber · O. Zaric
Department of Biomedical Imaging and Image-guided Therapy, MR Centre of Excellence, Medical University Vienna, Vienna, Austria

O. Abeyakoon
Department of Radiology, King's College, London, UK

P. Dubsky
Department of Surgery, Medical University Vienna, Vienna, Austria

Z. Bago-Horvath
Department of Pathology, Medical University Vienna, Vienna, Austria

Introduction

Dynamic contrast-enhanced magnetic resonance imaging (DCE-MRI) of the breast is an established, routinely used imaging investigation for the diagnosis and staging of breast cancer [1–6]. It has been demonstrated that utilization of high-resolution DCE-MRI protocols, which enable a detailed assessment of lesion morphology and enhancement kinetics, are beneficial for diagnostic accuracy [1, 7–9]. However, owing to restrictions in signal-to-noise ratio (SNR) the achievable temporal and spatial resolution at field strengths of 1.5 T or

less is limited. Hence an accurate assessment of very small lesions and non-mass-like enhancing lesions (NMLE) is difficult [10–12]. The use of parallel imaging and 3-T systems with an intrinsically higher SNR makes improvements in spatial and temporal resolution possible, facilitating a further increase in diagnostic accuracy [13–18]. Recently, ultra-high-field MR systems, operating at 7 T, have become available. In comparison to 1.5 T and 3 T, 7 T offers a further increase in intrinsic SNR, which can be translated into higher temporal and spatial resolution imaging [19–22] as well as functional and metabolic imaging [20, 23, 24]. Initial studies investigating unilateral DCE-MRI of the breast at 7 T demonstrated the feasibility in healthy volunteers and a few patients and encouraged the implementation of further advanced bilateral coil concepts to fully explore the putative diagnostic potential of DCE-MRI at 7 T [19, 20, 25, 26].

However, to date there is no experience with bilateral DCE-MRI of the breast at 7 T, and thus a translation from experimental to clinical imaging is warranted.

The aim of this study was to evaluate the clinical application of bilateral high temporal and spatial resolution (HR) DCE-MRI of the breast at 7 T with histopathology as the standard of reference.

Materials and methods

Patients

This prospective, single-centre study was approved by the ethics committee of our institution. Written, informed consent was obtained from all patients. From December 2011 until December 2012, 27 consecutive patients who fulfilled the following inclusion criteria were enrolled in the study: 18 years or older; not pregnant; not breastfeeding; an abnormality at mammography or breast ultrasound (asymmetric density, architectural distortion, suspicious microcalcification, or breast mass classified according to BI-RADS® category 0 or 4–5); no previous treatment, i.e. breast biopsy before MRI, neoadjuvant chemotherapy; and no contraindications to MRI or MR contrast agents [1]. In only one patient, the MR examination had to be aborted owing to ultra-high-field-induced severe nausea, and three patients could not participate owing to previously unknown claustrophobia. After exclusion of these patients, a total of 23 patients (age range, 25–82; mean age, 51.2) were included in the study. Regardless of the results of HR DCE-MRI imaging of the breast at 7 T, all lesions were histopathologically verified.

The initial BI-RADS® category distributions of the lesions before MRI were BI-RADS® 0 for 10 patients, BI-RADS® 4 for three patients and BI-RADS® 5 for 10 patients.

MRI

All patients underwent bilateral HR DCE-MRI of the breast in the prone position using a 7-T MR system (Magnetom, Siemens Healthcare, Erlangen, Germany) and a dedicated four-channel double-tuned $^{31}P/^{1}H$ breast coil (Stark Contrast, MRI Coils Research, Erlangen, Germany). In premenopausal women, HR DCE-MRI was performed in the second week of the menstrual cycle to minimize background parenchymal enhancement [1, 27, 28].

The following MRI sequence was performed in all patients: a transversal T1-weighted time-resolved angiography with stochastic trajectories sequence (TWIST), with spectral fat-saturation, a 0.7-mm isotropic voxel size and a temporal resolution of 14 s (TR/TE 4.8 ms/2.5 ms; FOV 196×330 mm^2; 176 slices, matrix 266×449; one average; centre k-space region with full reacquired 23 %; reacquisition density of peripheral k-space 20 %; temporal interpolation factor 2; TA 9 min). The TWIST sequence simultaneously allows both high temporal and spatial resolution MRI [4, 29, 30]. All patients received a single dose (0.1 mmol/kg body weight) of the contrast agent gadoterate meglumine (Gd-DOTA; Dotarem®, Guerbet, France) intravenously as a bolus, followed by a 20-ml saline flush administered manually. Application of contrast agent was started after three baseline MR data acquisitions.

Data analysis

All bilateral HR DCE-MRI data were prospectively and independently evaluated by two experienced breast radiologists (r1, 8 years of experience in breast MRI and r2, 11 years of experience in breast MRI) and a less experienced breast radiologist (final year resident with 1 year of experience in breast MRI, r3), who were all trained at different institutions. All readers were aware that the patients had a breast lesion, but they were not provided with the previous imaging or the histopathological results.

Lesions

Lesion size was measured using the largest diameter in one plane. HR DCE-MRI imaging data was assessed using the descriptors defined in the American College of Radiology (ACR) MRI BI-RADS® lexicon. Lesions were classified as masses or non-mass-like enhancement (NMLE).

According to the ACR MRI BI-RADS® lexicon, the following descriptors were assessed for masses: shape (round, oval, lobulated, irregular); margin (smooth, irregular, spiculated); enhancement pattern (homogenous, heterogeneous); and enhancement kinetics [31] [persistent enhancement (type I), initial strong enhancement and plateau-phase (type II), initial strong enhancement and washout (type III)].

For NMLE, the distribution (focal, regional, multiple regions, segmental, ductal, linear and diffuse), the pattern of enhancement (homogenous, heterogeneous, clumped and stippled) and the symmetry were assessed. For the assessment of the enhancement kinetics of masses, regions of interest (ROIs) were manually drawn in the most enhancing part of the tumour and time–signal intensity curves were calculated [32, 33]. For NMLE, the enhancement kinetics were not taken into account [9, 10, 13, 14]. Using the descriptors as defined by BI-RADS®, an interpretation scheme based on the BI-RADS® classification system introduced by Kuhl et al. [9] and implemented by Pinker et al. [13, 14] was used to estimate the probability of malignancy for each lesion.

Image quality

All bilateral HR DCE-MR images were independently assessed and graded on a scale from 1 to 5 by two readers independently.

Overall image quality, lesion conspicuity and quality of fat-suppression were graded as 1 (excellent), 2 (good), 3 (moderate), 4 (poor) or 5 (insufficient).

B1-field heterogeneity and presence of artefacts, e.g. motion artefacts, wrap around artefacts or chemical shift artefacts, were graded as 1 (none), 2 (mild), 3 (moderate), 4 (severe) or 5 (insufficient). The criteria for image quality was lesion-based i.e. we assessed the quality of the above parameters surrounding the lesions. This was done in order to reflect the diagnostic quality of the obtained images as a general image quality rating would not take into account regional deterioration of images which could lead to misinterpretation.

Histopathology

In all patients, the final diagnosis was established by histopathology by one pathologist, using either image-guided needle biopsy or surgery [34]. In the case of a benign histopathological diagnosis at image-guided needle biopsy, the final diagnosis was benign ($n=9$). In the case of a high-risk lesion, which had an uncertain potential for malignancy, the final diagnosis was established with open surgery ($n=1$) [35] Table 1.

Statistical methods

Statistical analysis was performed by a statistician (M.W.), using SPSS 19.0 and CIA 2.2.0. All calculations were performed on a per lesion basis. To calculate the sensitivity and specificity of bilateral HR DCE-MRI of the breast at 7 T, the assigned final MR BI-RADS® classifications were dichotomized. BI-RADS® 1–3 were considered benign. BI-RADS® 4 and 5 were considered malignant. Sensitivity, specificity, accuracy, negative predictive value (NPV), positive predictive value (PPV), the area under the curve (AUC) and 95 % confidence intervals (CI) for HR DCE-MRI of the breast at 7 T were calculated. Histopathology was used as the standard of reference. Inter-reader variability was assessed by κ coefficients.

Table 1 Detailed histopathological diagnoses

Malignant	*n*
	19
Histopathological subtype	
3IDC	14
ILC	4
DCIS	1
Benign	*n*
	10
Histopathological subtype	
High risk (papilloma with atypia)	1
FA/FAH	8
Focal fibrosis	1

IDC invasive ductal carcinoma, *ILC* invasive lobular carcinoma, *DCIS* ductal carcinoma in situ, *FA* fibroadenoma, *FAH* fibroadenomatous hyperplasia

Results

A total of 29 lesions ranging from 8 to 47 mm (mean 23.9 mm) were detected in 23 patients. There were 24 enhancing masses (size range 9–47 mm, mean 22.1 mm) and five NMLE (size range 8–44 mm, mean 34.4 mm). Histopathology revealed 19 malignant and ten benign lesions (Table 1). The frequency of each BI-RADS® descriptor for benign and malignant lesions and all readers is given in Table 2.

All readers classified eight lesions as MR BI-RADS® 2, one lesion as MR BI-RADS® 3, two lesions as MR BI-RADS® 4 and 18 lesions MR BI-RADS® 5. On the basis of the dichotomization rules, bilateral HR DCE-MRI of the breast at 7 T determined 20 lesions to be malignant (Figs. 1 and 3) and nine lesions to be benign (Fig. 2).

Bilateral HR DCE-MRI of the breast at 7 T achieved a sensitivity of 100 % (19 out of 19 lesions, 95 % CI 83.2–100 %) and a specificity of 90 % (9 out of 10 lesions, 95 % CI 59.6–98.2 %), resulting in a diagnostic accuracy of 96.6 % (28 out of 29 lesions, 95 % CI 82.8–99.4 %), with an AUC of 0.95 (95 % CI 0.839–1). The PPV was 95 % (19 out of 20 lesions), with a 95 % CI of 76.4–99.1 %, and the NPV was 100 % (9 out of 9 lesions), with a 95 % CI of 70.1–100 %. There was no disagreement between all three readers regarding lesions classification.

There were no false-negative lesions and one false-positive lesion. The false-positive lesion was a fibroadenomatous

Table 2 Frequency of BI-RADS® descriptors for benign and malignant lesions and all readers

Shape						
Oval				2	2	2
Irregular	15	15	15	1	1	1
Lobulated				6	6	6
Margin						
Irregular	8	8	8	1	1	1
Smooth				8	8	8
Spiculated	7	7	7			
Internal EH pattern						
Homogeneous	1	1	1	6	6	6
Heterogeneous	13	13	13	1	1	1
Dark internal septations				2	2	2
Rim EH	1	1	1			
Kinetics						
Persistent				6	6	6
Plateau	8	8	8	3	3	3
Washout	7	7	7			
NMLE	$n = 4$		$n = 1$			
	r1	r2	r3	r1	r2	r3
Distribution						
Regional	3	3	3	1	1	
Segmental	1	1	1			
Internal EH pattern						
Heterogeneous	2	2	2	1	1	1
Clumped	1	1	1			
Symmetry						
Asymmetric	3	3	3	1	1	1
Shape						
Oval				2	2	2
Irregular	15	15	15	1	1	1
Lobulated				6	6	6
Margin						
irregular	8	8	8	1	1	1
Smooth				8	8	8
Spiculated	7	7	7			
Internal EH pattern						
Homogeneous	1	1	1	6	6	6
Heterogeneous	13	13	13	1	1	1
Dark internal septations				2	2	2
Rim EH	1	1	1			
Kinetics						
Persistent				6	6	6
Plateau	8	8	8	3	3	3
Washout	7	7	7			
NMLE	$n = 4$			$n = 1$		
	r1	r2	r3	r1	r2	r3
Distribution						
Regional	3	3	3	1	1	
Segmental	1	1	1			
Internal EH pattern						
Heterogeneous	2	2	2	1	1	1
Clumped	1	1	1			
Symmetry						
Asymmetric	3	3	3	1	1	1

BI-RADS® Breast Imaging Reporting and Data System, *EH* enhancement, *NMLE* non-mass-like enhancement

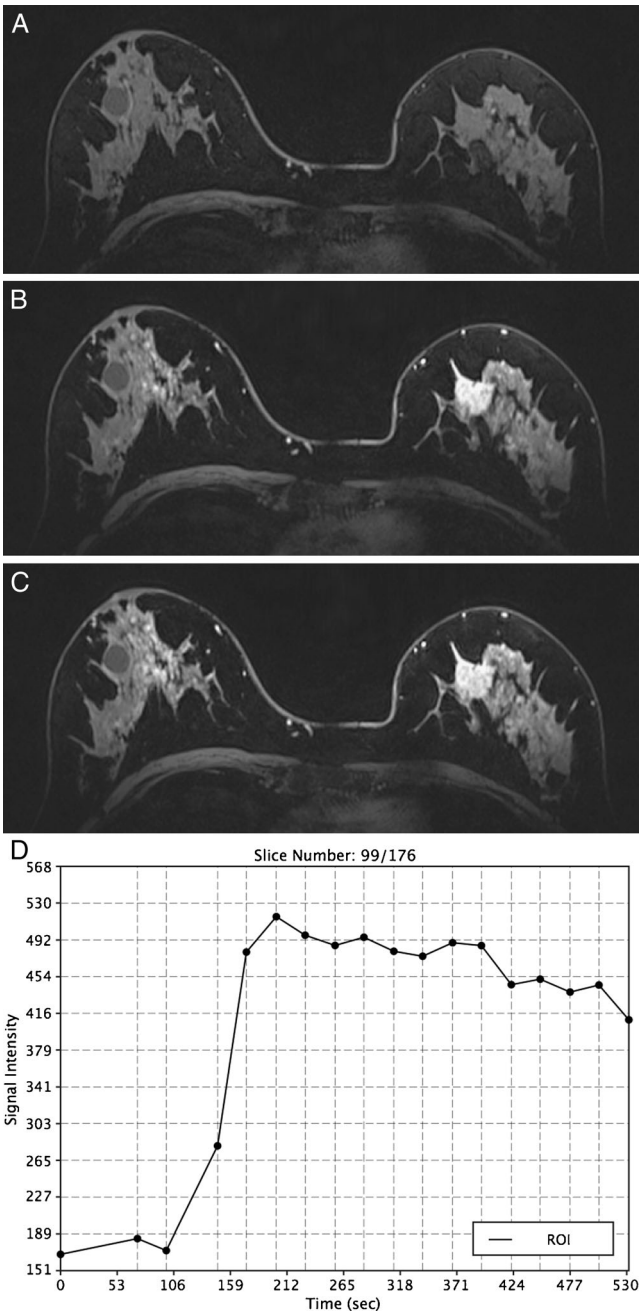

Fig. 1 Invasive ductal carcinoma G3 in a 63-year-old woman, centrally in the left breast. **a**–**d** The irregular-shaped mass with spiculated margins demonstrates slightly heterogeneous initial strong enhancement followed by a washout, and was classified as BI-RADS© 5 (highly suggestive of malignancy) by all readers

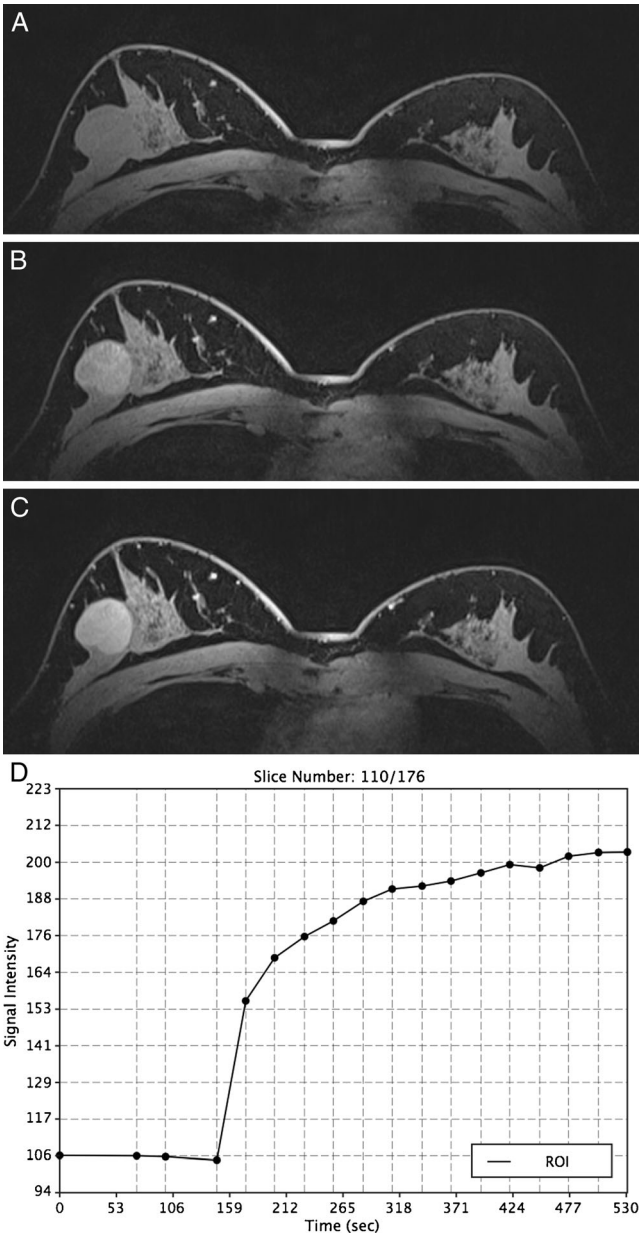

Fig. 2 Fibroadenoma in a 32-year-old woman at the 3 o'clock position of the right breast. **a**–**d** The lobulated mass with smooth margins demonstrated a persistent enhancement and non-enhancing septa, and was, therefore, correctly classified as BI-RADS© 2 (benign) by all readers

hyperplasia, which demonstrated an irregular shape and margin and type II enhancement kinetics.

There was excellent inter-reader agreement for all three readers for the BI-RADS® descriptors ($\kappa=1$), artefacts ($\kappa=1$), lesion conspicuity ($\kappa<0.89$), homogeneity of signal ($\kappa=1$), fat suppression ($\kappa=1$) and overall image quality ($\kappa=1$).

All examinations were diagnostic and were not hampered by artefacts. Overall image quality was scored excellent in $n=27$ (r1), n=27 (r2) and $n=27$ (r3), good in $n=1$ (r1), $n=1$ (r2) and $n=1$ (r3) and moderate in $n=1$ (r1), $n=1$ (r2) and $n=1$ (r3). Complete results regarding image quality, i.e.

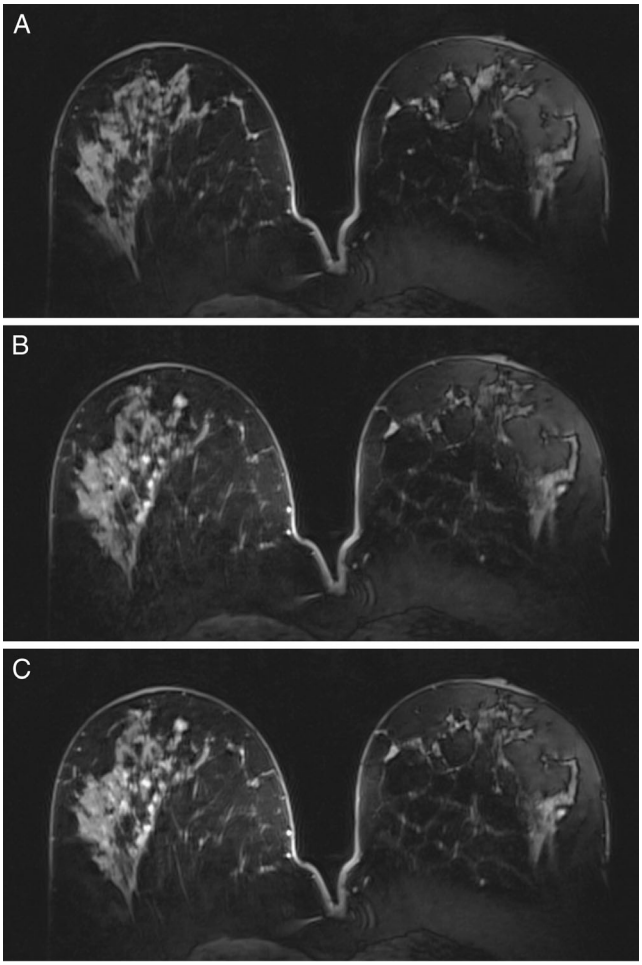

Fig. 3 High-grade ductal carcinoma in situ in a 55-year-old woman, centrally in the right breast. **a**–**c** HR DCE-MRI of the breast at 7 T shows an asymmetric, regional, clumped, non-mass-like enhancement centrally in the right breast, which is correctly classified as BI-RADS© 4 (suspicious) by all readers

overall image quality, B1-field inhomogeneity, quality of fat suppression and presence of artefacts, are depicted in Table 3.

Discussion

Our study demonstrates that bilateral HR DCE-MRI of the breast at 7 T is clinically applicable. To our knowledge, this work presents the first patient series examined with bilateral HR DCE-MRI of the breast at 7 T. Using an MRI sequence with an isotropic spatial resolution of 0.7 mm and a high temporal resolution of 14 s, a detailed depiction of lesion morphology and assessment of lesion enhancement kinetics is feasible enabling an accurate breast cancer diagnosis with an AUC of 0.95, excellent inter-reader agreement ($\kappa=0.89$–1) and image quality.

There have been previous reports on breast MRI at 7 T. An initial study by Umutlu et al. investigated the feasibility of unilateral DCE-MRI at 7 T using a unilateral, single-loop coil

Table 3 Detailed results of image quality for both readers

	Readers			κ agreement		
	r1	r2	r3	r1 vs r2	r1 vs r3	r2 vs r3
Overall image quality				1	1	1
Excellent	27	27	27			
Good	1	1	1			
Moderate	1	1	1			
Poor						
Insufficient						
Lesion conspicuity				0.89	0.93	1
Excellent	24	24	24			
Good	2	1	1			
Moderate	3	4	4			
Poor						
Insufficient						
B1-field heterogeneity				1	1	1
None	28	28	28			
Mild	1	1	1			
Moderate						
Severe						
Insufficient						
Quality of fat suppression				1	1	1
Excellent	26	26	26			
Good	2	2	2			
Moderate	1	1	1			
Poor						
Insufficient						
Artefacts				1	1	1
None	28	28	28			
Mild	1	1	1			
Moderate						
Severe						
Insufficient						

in ten healthy volunteers and five patients with breast cancer. The authors concluded that DCE-MRI of the breast is possible, yet challenging, and further improvements were necessary to circumvent the limitations of the coil design and the ultra-high magnetic field strength [25].

Brown et al. demonstrated in another volunteer study (without the use of contrast agents) that improvements in coil design now facilitate bilateral high-resolution 3D gradient echo imaging with an image quality as good as, or better than, 3 T [21].

Korteweg et al. evaluated the feasibility of unilateral DCE-MRI at 7 T in five healthy volunteers and three patients with advanced breast cancer, and reported encouraging results. The authors demonstrated that, compared to 3 T, a substantial increase in SNR, as well as functional imaging strategies, such as diffusion-weighted imaging and proton MR spectroscopy, are possible, and that 7-T MRI of the breast has a putative diagnostic potential [20]. Stehouwer et al., who investigated unilateral DCE-MRI of the breast at 7 T in comparison to 3 T, confirmed these findings and concluded that DCE-MRI of the breast at 7 T yields results that are at least comparable to those obtained at 3 T [26]. In a recent study, Stehouwer et al. confirmed previous results regarding unilateral DCE-MRI with a temporal resolution of 63 s and a spatial resolution of $1\times1\times2$ mm. Additionally, the authors performed an ultra-high-resolution T1-weighted sequence with a spatial resolution $0.45\times0.57\times0.45$ with an acquisition time of 13 min 32 s [22].

Van de Bank et al. also reported initial results on unilateral HR DCE-MRI of the breast at 7 T. In that study, the authors examined six healthy volunteers and one patient, and proved that the acquisition of an interleaved dynamic, contrast-enhanced MRI protocol, consisting of ultra-high spatial resolution (0.6 mm isotropic voxel size, 69 s) and ultra-high temporal resolution (1.5 mm isotropic voxel size, 6.7 s), is feasible. The authors concluded that DCE-MRI, including both high temporal and spatial resolution, has the potential to increase specificity in the detection and grading of breast cancer [19].

As opposed to all previous studies, we employed a bilateral simultaneous high temporal (14 s) and high spatial (0.7 mm isotropic) DCE-MRI protocol for breast lesion diagnosis in patients with a total study time of 9 min. With regards to temporal and spatial resolution as well as image quality, the presented technique outperforms all previously presented protocols at any given field strength.

We demonstrated that bilateral HR DCE-MRI at 7 T is clinically applicable, and owing to an increase in SNR an accurate assessment of lesion morphology and enhancement kinetics is facilitated. Initial studies reported challenges due to imaging artefacts associated with the ultra-high field [25]. However, recent studies demonstrated that, with improvements in coil design and software, these limitations could be overcome [19, 20, 26]. This is in good agreement with the results of the current study. All bilateral HR DCE-MRI were diagnostic and not hampered by imaging artefacts associated with the ultra-high field.

Although in this study bilateral HR DCE-MRI of the breast at 7 T detected all breast cancer lesions, there remained one false-positive lesion. The false-positive lesion was a fibroadenomatous hyperplasia, which demonstrated an irregular shape and margins, as well as type III enhancement kinetics and was rated as BI-RADS® 5 by both experienced readers independently. This highlights the inherent limitations of bilateral HR DCE-MRI and the potential of functional imaging strategies such as DWI and spectroscopy, which benefit from the increased SNR at 7 T [20, 23, 24].

A limitation of our study is the small number of ductal carcinomas in situ (DCIS) and invasive lobular carcinomas (ILC) compared to invasive ductal carcinomas (IDC) in our

patient collective, and the fact that the DCIS was high grade. The excellent results for both ILC [36–38] and high-grade DCIS seen in this study are in accordance with previously published reports [39, 40]. Further studies that include larger numbers of patients will be needed to verify these results. In the present study we focused on T1-weighted bilateral HR DCE-MRI of the breast only. International recommendations suggest including T2-weighted imaging in order to improve diagnostic confidence of breast MRI [1, 41]. However, there is only little evidence on the diagnostic benefit of T2-weighted images [42]. Owing to restrictions of specific absorption rate (SAR) limits, spin echo derived T2-weighted imaging at 7 T is challenging. A potential solution to circumvent SAR limit restrictions could be the use of echo planar imaging derived T2-weighted images [30]. Another limitation of our study is that no direct comparison with bilateral HR DCE-MRI of the breast at 3 T was performed, and therefore, a potential increase in diagnostic accuracy cannot be assessed. Such a comparison is demanding in terms of patients to be included. In order to prove a diagnostic superiority of either sensitivity or specificity of 10 % with alpha and beta errors defined to 5 % and 20 %, respectively, 71 patients per group have to be examined. Because 3-T MRI has shown excellent diagnostic parameters [13, 14], such major differences in diagnostic performance are not to be expected. However, owing to the achievable higher spatial and temporal resolution, an improvement in diagnosis of small and non-mass-like lesions, which currently pose a problem to DCE-MRI of the breast, can be expected [10, 12]. Additionally, the aim of this study was to prove the feasibility of HR DCE-MRI of the breast at 7 T in clinical practice, which was demonstrated. In addition, both readers in this study were expert breast radiologists with extensive training in DCE-MRI, which might have influenced the excellent results regarding diagnostic accuracy and inter-reader agreement.

Bilateral HR DCE-MRI of the breast at 7 T is clinically applicable and the results of this study indicate that accurate breast cancer diagnosis with excellent inter-rater agreement independent of experience and image quality should be feasible.

Acknowledgments Funding was provided by the Austrian Nationalbank 'Jubiläumsfond' Project 5082.

References

1. Sardanelli F, Boetes C, Borisch B et al (2010) Magnetic resonance imaging of the breast: recommendations from the EUSOMA working group. Eur J Cancer 46:1296–1316
2. Turnbull LW (2009) Dynamic contrast-enhanced MRI in the diagnosis and management of breast cancer. NMR Biomed 22:28–39
3. Orel SG, Schnall MD (2001) MR imaging of the breast for the detection, diagnosis, and staging of breast cancer. Radiology 220: 13–30
4. Schnall M, Orel S (2006) Breast MR imaging in the diagnostic setting. Magn Reson Imaging Clin N Am 14:329–337, vi
5. Morrow M, Waters J, Morris E (2011) MRI for breast cancer screening, diagnosis, and treatment. Lancet 378:1804–1811
6. DeMartini W, Lehman C (2008) A review of current evidence-based clinical applications for breast magnetic resonance imaging. Top Magn Reson Imaging 19:143–150
7. Kinkel K, Helbich TH, Esserman LJ et al (2000) Dynamic high-spatial-resolution MR imaging of suspicious breast lesions: diagnostic criteria and interobserver variability. AJR Am J Roentgenol 175: 35–43
8. Liberman L, Morris EA, Lee MJ et al (2002) Breast lesions detected on MR imaging: features and positive predictive value. AJR Am J Roentgenol 179:171–178
9. Kuhl CK, Schild HH, Morakkabati N (2005) Dynamic bilateral contrast-enhanced MR imaging of the breast: trade-off between spatial and temporal resolution. Radiology 236:789–800
10. Baltzer PA, Benndorf M, Dietzel M, Gajda M, Runnebaum IB, Kaiser WA (2010) False-positive findings at contrast-enhanced breast MRI: a BI-RADS descriptor study. AJR Am J Roentgenol 194:1658–1663
11. Dietzel M, Baltzer PA, Vag T et al (2010) Differential diagnosis of breast lesions 5 mm or less: is there a role for magnetic resonance imaging? J Comput Assist Tomogr 34:456–464
12. Gutierrez RL, DeMartini WB, Eby PR, Kurland BF, Peacock S, Lehman CD (2009) BI-RADS lesion characteristics predict likelihood of malignancy in breast MRI for masses but not for nonmasslike enhancement. AJR Am J Roentgenol 193:994–1000
13. Pinker K, Grabner G, Bogner W et al (2009) A combined high temporal and high spatial resolution 3 Tesla MR imaging protocol for the assessment of breast lesions: initial results. Invest Radiol 44: 553–558
14. Pinker-Domenig K, Bogner W, Gruber S et al (2012) High resolution MRI of the breast at 3 T: which BI-RADS(R) descriptors are most strongly associated with the diagnosis of breast cancer? Eur Radiol 22:322–330
15. Elsamaloty H, Elzawawi MS, Mohammad S, Herial N (2009) Increasing accuracy of detection of breast cancer with 3-T MRI. AJR Am J Roentgenol 192:1142–1148
16. Schmitz AC, Peters NH, Veldhuis WB et al (2008) Contrast-enhanced 3.0-T breast MRI for characterization of breast lesions: increased specificity by using vascular maps. Eur Radiol 18:355–364
17. Kuhl CK, Jost P, Morakkabati N, Zivanovic O, Schild HH, Gieseke J (2006) Contrast-enhanced MR imaging of the breast at 3.0 and 1.5 T in the same patients: Initial experience. Radiology 239:666–676
18. Rahbar H, Partridge SC, DeMartini WB, Thursten B, Lehman CD (2013) Clinical and technical considerations for high quality breast MRI at 3 Tesla. J Magn Reson Imaging 37:778–790
19. van de Bank BL, Voogt IJ, Italiaander M et al (2012) Ultra high spatial and temporal resolution breast imaging at 7 T. NMR Biomed. doi:10.1002/nbm.2868
20. Korteweg MA, Veldhuis WB, Visser F et al (2011) Feasibility of 7 Tesla breast magnetic resonance imaging determination of intrinsic sensitivity and high-resolution magnetic resonance imaging, diffusion-weighted imaging, and (1)H-magnetic resonance spectroscopy of breast cancer patients receiving neoadjuvant therapy. Invest Radiol 46:370–376
21. Brown R, Storey P, Geppert C et al (2013) Breast MRI at 7 Tesla with a bilateral coil and T1-weighted acquisition with robust fat suppression: image evaluation and comparison with 3 Tesla. Eur Radiol 23: 2969–2978
22. Stehouwer BL, Klomp DW, van den Bosch MA et al (2013) Dynamic contrast-enhanced and ultra-high-resolution breast MRI at 7.0 Tesla. Eur Radiol 23:2961–2968

23. Wijnen JP, van der Kemp WJ, Luttje MP, Korteweg MA, Luijten PR, Klomp DW (2011) Quantitative (31) P magnetic resonance spectroscopy of the human breast at 7 T. Magn Reson Med 68:339–348
24. Klomp DW, van de Bank BL, Raaijmakers A et al (2011) 31P MRSI and 1H MRS at 7 T: initial results in human breast cancer. NMR Biomed 24:1337–1342
25. Umutlu L, Maderwald S, Kraff O et al (2010) Dynamic contrast-enhanced breast MRI at 7 Tesla utilizing a single-loop coil: a feasibility trial. Acad Radiol 17:1050–1056
26. Stehouwer BL, Klomp DW, Korteweg MA et al (2013) 7 T versus 3 T contrast-enhanced breast magnetic resonance imaging of invasive ductulolobular carcinoma: first clinical experience. Magn Reson Imaging 31:613–617
27. Baltzer PA, Dietzel M, Vag T et al (2011) Clinical MR mammography: impact of hormonal status on background enhancement and diagnostic accuracy. RöFo 183:441–447
28. DeMartini WB, Liu F, Peacock S, Eby PR, Gutierrez RL, Lehman CD (2012) Background parenchymal enhancement on breast MRI: impact on diagnostic performance. AJR Am J Roentgenol 198: W373–W380
29. Han BK, Schnall MD, Orel SG, Rosen M (2008) Outcome of MRI-guided breast biopsy. AJR Am J Roentgenol 191:1798–1804
30. Solin LJ, Orel SG, Hwang WT, Harris EE, Schnall MD (2008) Relationship of breast magnetic resonance imaging to outcome after breast-conservation treatment with radiation for women with early-stage invasive breast carcinoma or ductal carcinoma in situ. J Clin Oncol 26:386–391
31. Kuhl CK, Mielcareck P, Klaschik S et al (1999) Dynamic breast MR imaging: are signal intensity time course data useful for differential diagnosis of enhancing lesions? Radiology 211:101–110
32. Insko EK, Connick TJ, Schnall MD, Orel SG (1997) Multicoil array for high resolution imaging of the breast. Magn Res Med 37:778–784
33. Solomon B, Orel S, Reynolds C, Schnall M (1998) Delayed development of enhancement in fat necrosis after breast conservation therapy: a potential pitfall of MR imaging of the breast. AJR Am J Roentgenol 170:966–968
34. Schueller G, Jaromi S, Ponhold L et al (2008) US-guided 14-gauge core-needle breast biopsy: results of a validation study in 1352 cases. Radiology 248:406–413
35. Degnim AC, King TA (2013) Surgical management of high-risk breast lesions. Surg Clin North Am 93:329–340
36. Mann RM, Veltman J, Huisman H, Boetes C (2011) Comparison of enhancement characteristics between invasive lobular carcinoma and invasive ductal carcinoma. J Magn Reson Imaging 34:293–300
37. Mann RM, Loo CE, Wobbes T et al (2010) The impact of preoperative breast MRI on the re-excision rate in invasive lobular carcinoma of the breast. Breast Cancer Res Treat 119:415–422
38. Weinstein SP, Orel SG, Heller R et al (2001) MR imaging of the breast in patients with invasive lobular carcinoma. AJR Am J Roentgenol 176:399–406
39. Kuhl CK, Schrading S, Bieling HB et al (2007) MRI for diagnosis of pure ductal carcinoma in situ: a prospective observational study. Lancet 370:485–492
40. Lehman CD (2010) Magnetic resonance imaging in the evaluation of ductal carcinoma in situ. J Natl Cancer Inst Monogr 2010:150–151
41. Mann RM, Kuhl CK, Kinkel K, Boetes C (2008) Breast MRI: guidelines from the European Society of Breast Imaging. Eur Radiol 18:1307–1318
42. Baltzer PA, Dietzel M, Kaiser WA (2011) Nonmass lesions in magnetic resonance imaging of the breast: additional T2-weighted images improve diagnostic accuracy. J Comput Assist Tomogr 35:361–366